Available online at www.sciencedirect.com
SCIENCE DIRECT®

Sensors and Actuators A 117 (2005) 186–193

SENSORS AND ACTUATORS A PHYSICAL
www.elsevier.com/locate/sna

Determining the in-plane and out-of-plane dynamic response of microstructures using pulsed dual-mode ultrasonic array transducers

Wen Pin Lai, Weileun Fang*

Power Mechanical Engineering Department, National Tsing Hua University, Hsinchu 30043, Taiwan

Received 10 June 2004; accepted 18 June 2004

Abstract

A novel dual-directional actuation technique to determinate the in-plane and out-of-plane dynamic response of the microstructure is presented in this study. The dual-mode ultrasonic array transducer has been realized to simultaneously generate the in-plane and the out-of-plane pulsed bulk acoustic waves (BAW). Thus the array transducer can be exploited to excite the micromachined structures. This array transducer, which acts as a vibration exciter during the vibration test, is named the dual-mode BAW hammer. The performance of the dual-direction hammer was designed and simulated by the commercial finite element analysis software. In application of this technique, the micromachined cantilevers were employed to conduct the vibration test. Experimental results showed that the in-plane and the out-of-plane vibration modes of micro beams were simultaneously excited using the dual-mode BAW hammer. Since the sample and the measurement apparatus are very simple, this approach has the potential for wafer level on-line testing.

Keywords: In-plane dynamic response; Microstructures; Dual-mode ultrasonic transducer; Impulse excitation

1. Introduction

Ultrasonic array transducers are widely used in medical diagnostic ultrasound imaging system [1–5]. The ultrasonic array transducer mainly consists of PZT array elements, backing layer, matching layer and lens layer. Because the operating frequency of the PZT element is close to the natural frequencies of microstructures, it is especially suitable for the application of MEMS testing. For instance, various harmonic excitation techniques are using PZT discs as the driving source to determine the dynamic response of microstructures [6–8]. In this manner, the measured natural frequencies of the microstructure may be shifted when they are near the resonance of the PZT discs. To avoid the interference of PZT dynamics during vibration test, a novel out-of-plane pulse generator is exploited to excite the microstructure [9]. Moreover, this impulse excitation test differs from the resonant approach [10] and swept sine method [7].

The vibration exciter (or shaker) is one of the primary considerations for the vibration test of passive micromachined structures. There are various existing vibration exciters, such as the PZT shaker [6–8], ultrasonic wave [9], optic thermal [10], and electrostatic force [11,12] for MEMS vibration test. However, these approaches can only excite micromachined structures to vibrate in the out-of-plane direction. Recently, various high aspect ratio microstructures employed as the in-plane actuators or sensors have been realized using different micromachining processes [13]. It becomes more important to determine the dynamic characteristics of microstructures along the in-plane direction. In other words, it is crucial to develop an appropriate shaker for the vibration test of passive micromachined structures. The in-plane motion of the microstructures can be driven using the built-in electrostatic electrodes or micromachined actuators [11,12]. However, it is necessary to deposit additional films or fabricate additional micromachined actuator.

This study investigated a dual-mode ultrasonic array transducer to simultaneously generate the in-plane and the out-of-plane pulsed bulk acoustic waves (BAW). Thus the array transducer can be exploited to apply dual-directional impulses to excite the micromachined structures. This array transducer, which acted as a vibration exciter during the vibration test, was named the dual-mode BAW hammer. After the impulse excitation, the in-plane and out-of-plane dynamic characteristics of the microstructure were measured

---

* Corresponding author. Tel.: +886-3-574-2923; fax: +886-3-574-2923.
E-mail address: fang@pme.nthu.edu.tw (W. Fang).

0924-4247/$ – see front matter © 2004 Elsevier B.V. All rights reserved.
doi:10.1016/j.sna.2004.06.010

using laser Doppler vibrometer (LDV). The dual-mode BAW hammer has been successfully designed and fabricated in this study to show its feasibility. In addition, the dynamic test of micromachined cantilevers using the dual-mode BAW hammer has also been demonstrated.

2. Designs and analysis

The dual-mode ultrasonic array transducer, which consisted of various PZT bars, is schematic illustrated in Fig. 1a. The array transducer will produce impulse responses correlated with its thickness extensional mode and lateral mode simultaneously after the PZT bars driven by a pulse voltage. During the vibration test, the lateral mode of the transducer can be employed to generate the in-plane excitation. In addition, the thickness extensional mode of the transducer can be employed to provide the out-of-plane excitation. Generally, the characteristics of the dual-direction BAW hammer including resonant frequency, bandwidth and amplitude are determined by the backing layer and the dynamics of PZT array. This study tuned the dynamic characteristic of the BAW hammer by varying the dimensions of the PZT bar. As indicated in Fig. 1b, the aspect ratio R of the PZT bar of width W and thickness T is expressed as $R = W/T$.

Since the PZT bars in Fig. 1b have the same dimensions and material, their dynamic characteristics are identical. To simplify the analytical model of the dual-mode BAW hammer, the vibration characteristic of a single PZT bar was studied first. Hence, the dynamic characteristics, such as the resonant frequencies, modal shapes, the impedance response, and the impulse response, of the dual-mode hammer were predicted. The commercial software ANSYS was employed in the analysis. A PZT rod with length $L = 14\,\text{mm}$ and thickness $T = 0.4\,\text{mm}$ was used as a typical study case for simulation. The material properties of the PZT bar are

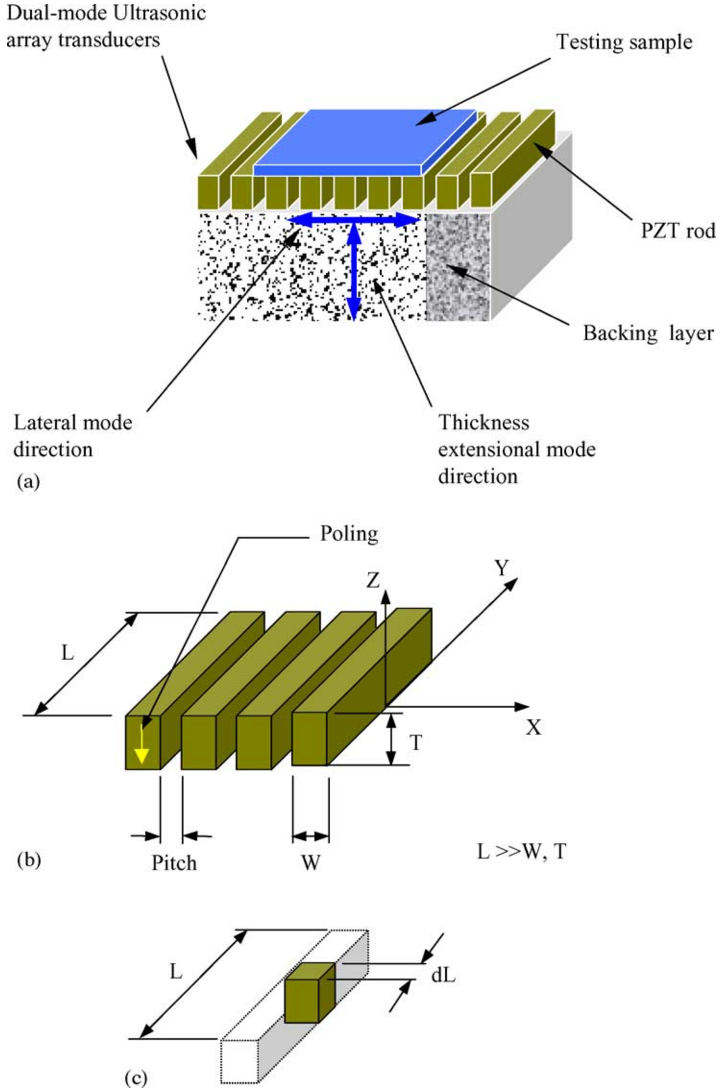

Fig. 1. A schematic diagram of BAW hammer: (a) the dual-mode bulk acoustic wave hammer using pulsed dual-mode ultrasonic array transducer; (b) PZT array bars; (c) the component used in the FEM model.

Table 1
Material properties of the PZT bars used for ANSYS simulation [14]

Density	$7750\,\mathrm{kg/m^3}$
Elastic constant	$C^{\mathrm{E}} = \begin{bmatrix} 121 & 7.54 & 7.52 & 0.0 & 0.0 & 0.0 \\ & 121 & 7.52 & 0.0 & 0.0 & 0.0 \\ & & 11.1 & 0.0 & 0.0 & 0.0 \\ & & & 2.11 & 0.0 & 0.0 \\ & & & & 2.11 & 0.0 \\ & & & & & 2.26 \end{bmatrix} \times 10^{10}\,\mathrm{N/m^2}$
Piezoelectric constant	$e = \begin{bmatrix} 0 & 0 & 0 & 0 & 12.3 & 0 \\ 0 & 0 & 0 & 12.3 & 0 & 0 \\ -5.4 & -5.4 & 15.8 & 0 & 0 & 0 \end{bmatrix} \mathrm{A\,s/m^2}$
Dielectric constant	$\varepsilon^s = \begin{bmatrix} 8.1066 & 0 & 0 \\ 0 & 8.1066 & 0 \\ 0 & 0 & 8.1066 \end{bmatrix} \times 10^{-9}\,\mathrm{A\,s/V\,m}$

listed in Table 1 [14]. The element type used in the analysis was SOLID 5. As shown in Fig. 1b, the length *L* of the PZT bars is far larger than the thickness *T* and width *W*. This study only considered the thickness extensional mode (in *Z*-direction) and lateral mode (in *X*-direction) of the PZT bar. The excitations and boundary conditions of the PZT bar were uniformly distributed along the *Y*-axis in Fig. 1b. Thus, a simplified FEM model with thickness *T*, width *W*,

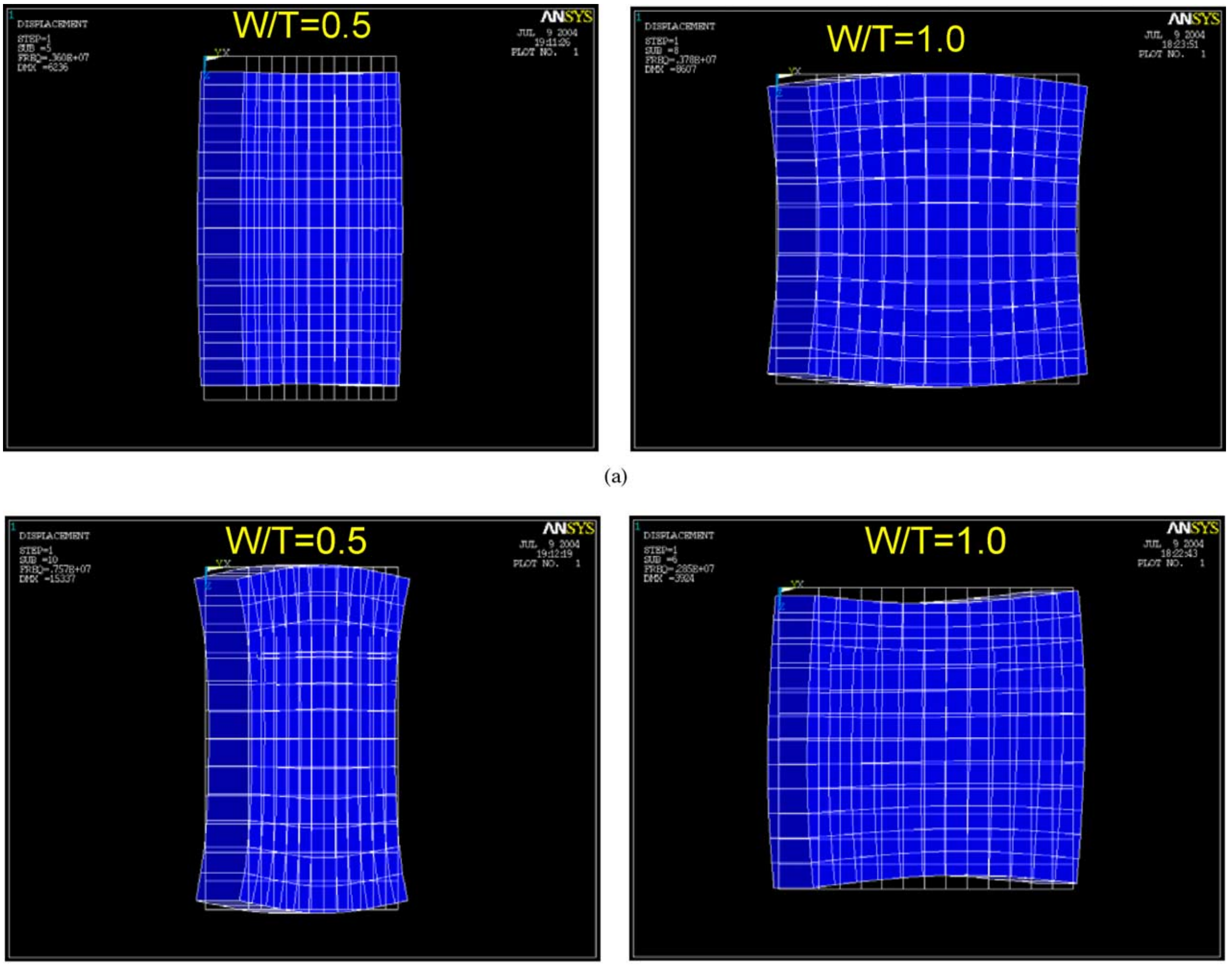

(a)

(b)

Fig. 2. The modal analysis results of the PZT bar for two different aspect ratios $R = 0.5$ and 1.0: (a) thickness mode; (b) lateral mode.

and length dL (d$L \ll L$) shown in Fig. 1c was established to reduce the computational time. The FEM models with element number ranging from 36 to 400 were analyzed to confirm the convergence of the results. The FEM results were converged if the element number was above 144. Therefore, the following simulation results of the PZT bar will be based on the FEM model with 144 mesh elements.

Fig. 2 shows the natural frequencies and mode shapes of the PZT bar associated with two different aspect ratios R. Fig. 2a demonstrates that the natural frequencies for thickness mode are 3.55 and 3.8 MHz, respectively, when the aspect ratio is $R = 0.5$ and 1, respectively. As shown in Fig. 2b, the natural frequencies of the lateral mode are 7.62 and 2.85 MHz when the aspect ratio is $R = 0.5$ and 1, respectively. The analysis shows that the modal frequency and mode shape of the PZT bar is strongly affected by the aspect ratio R. Moreover, the electrical impedance of the PZT was also predicted by the FEM analysis, as shown in Fig. 3. The natural frequencies were also obtained from this analysis. As indicated in Fig. 3, the natural frequencies of the PZT bar obtained from the impedance–frequency curve agree with those obtained from the modal analysis. According to the analysis, the thickness mode and lateral mode were approximate 4 MHz apart, and will not coupled with each other, when the aspect ratio $R = 0.5$. However, these two vibration modes were only 1 MHz apart, and could be coupled in a certain frequency range, when the aspect ratio $R = 1.0$.

Fig. 4 shows the simulated impulse waveform of the dual-mode BAW hammer when $R = 1.0$, and the driving voltage is 100 V. Since the shear acoustic wave velocity is slower than the bulk acoustic wave velocity, the first few cycles in Fig. 4a come from the thickness mode response and the rest come from the lateral mode response. The frequency spectrum associated with Fig. 4a is available in Fig. 4b. In short, the lateral and thickness extensional vibration modes of the dual-direction hammer tend to be coupled when the width and thickness of the PZT bar are closed (i.e. $R \approx 1.0$). If the characteristic of the array transducer is properly designed, these two orthogonal vibration modes will be simultaneously excited in one pulse excitation. Accordingly, a dual-mode BAW hammer is available from the array transducer with $R = 1.0$.

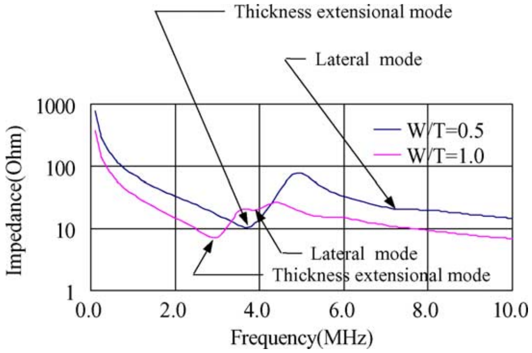

Fig. 3. The simulated electrical impedance of the PZT bars for $R = 0.5$ and 1.0.

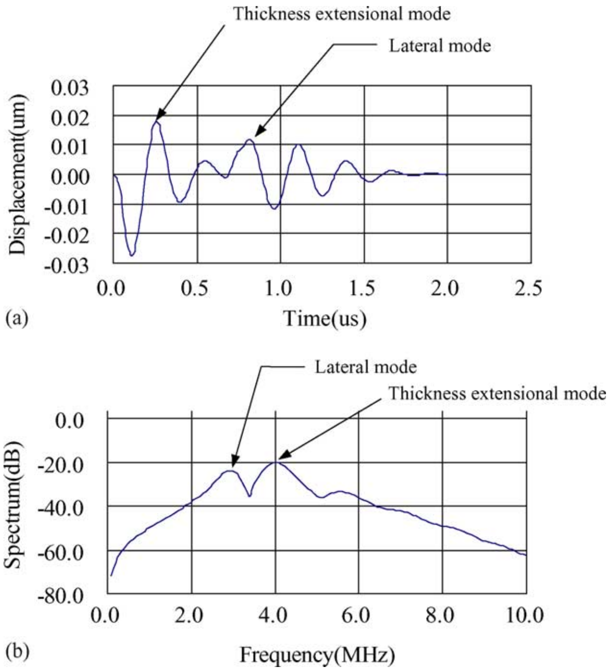

Fig. 4. The simulated impulse response of the BAW hammer for $R = 1.0$: (a) impulse time response; (b) impulse frequency response.

The micromachined cantilevers were employed as the test structures in this study. A cantilever beam with length $B_L = 80\,\mu$m, width $B_w = 5.3\,\mu$m, and thickness $t = 1.1\,\mu$m was selected as a typical study case. According to the modal analysis, the dynamic characteristics of the micro beam are shown in Fig. 5 and Table 2. Fig. 5 shows the mode shapes of the cantilever associated with its first six natural frequencies. In addition to the first four out-of-plane bending modes, these results also include the first in-plane bending mode and the first twisting mode. The vibration frequencies of these six modes are ranging from 126 kHz to 4.49 MHz, as listed in Table 2. To this end, the specific frequency range of the BAW hammer was designed in accordance with the dynamic response of the microstructures.

3. Experiments and discussion

The manufacturing processes of the dual-mode array transducer employed in this study are illustrated in Fig. 6. Firstly, a bulk PZT was diced to define the width and pitch of the array transducer, as shown in Fig. 6a and b. As depicted in Fig. 6c, the cables for signal and ground were connected to the PZT rods using soldering technique. Finally, the array transducer was fixed inside a housing after casting with the backing layer, as shown in Fig. 6d. To prepare the test samples, silicon dioxide cantilevers were fabricated on the (1 0 0) oriented silicon substrate using bulk micromachining. The thermal oxide film was grown on the (1 0 0) wafer and then patterned by buffered HF after

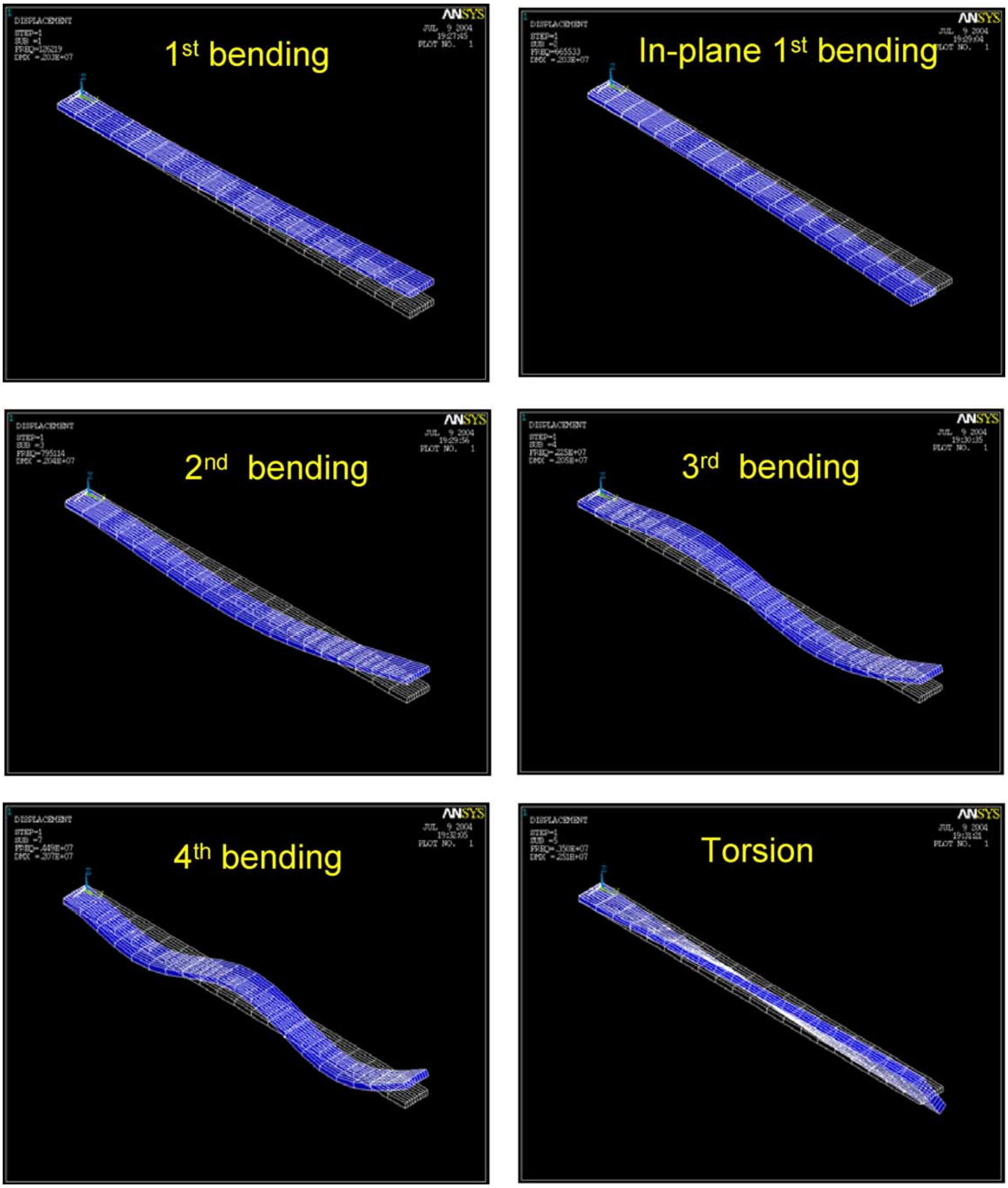

Fig. 5. The simulated resonant frequencies of the micro cantilever with 1.1 μm thick, 5.3 μm wide, and 80 μm long.

Table 2
Comparison of the simulation and experiments result of resonant frequencies of the micro beam with 1.1 μm thick, 5.3 μm wide, 80 μm long

Modal frequency	Out-of-plane first bending mode kHz	In-plane first bending mode kHz	Out-of-plane second bending mode kHz	Out-of-plane third bending mode MHz	Out-of-plane fourth bending mode MHz
Simulation result	126	666	794	2.25	4.49
Experiment result	130	620	770	2.29	4.62
Error percentage (%)	3	7.4	3.1	1.7	2.8

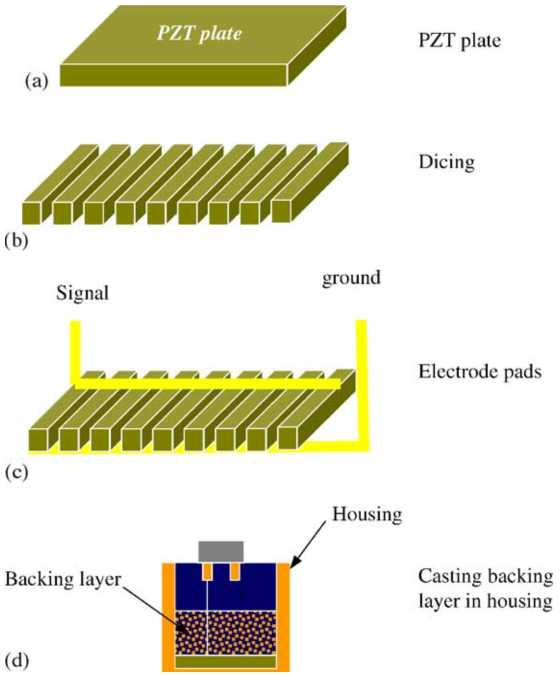

Fig. 6. The manufacturing process of the dual-mode BAW hammer.

photolithography. The micromachined silicon dioxide cantilevers were free suspended after the substrate underneath was etched anisotropically by the TMAH solution.

The experimental set-up for recording the dynamic response of microstructures using the dual-mode BAW hammer technique is illustrated in Fig. 7. The sample was mounted on the dual-mode ultrasonic array transducer by wax or sticky tape. The high voltage pulse generator system in Fig. 7 was used to produce a very short pulse voltage to drive the ultrasonic array transducer. Afterwards, the sample experienced a broad bandwidth frequency range excitation. Finally, the dynamic response of the microstructures was measured from the laser Doppler vibrometer (LDV) system. The time and frequency response of the microstructures was recorded and analyzed in the oscilloscope and spectrum analyzer. The insect of Fig. 7 shows the photograph of various micromachined cantilevers as the test sample. To compare with the analytical results, the test micromachined cantilevers were also 5.3 μm wide and 1.1 μm thick, and their length ranging from 20 to 80 μm. The gap between micro cantilevers and the substrate was 55 μm after the bulk etching to prevent the squeeze film effect.

The characteristics of the dual-mode BAW hammer would significantly affect the testing result of the microstructure. The performance of the dual-mode BAW hammer correlated closely with the design of the pulse generator and transducer. In the experiment, the amplitude of the driving voltage and the pulse repetition rate were well controlled by a commercial pulse generator. The pulse generator had an output impedance of 50 Ω. The pulse applied on the ultrasonic array transducer was 100 V in amplitude, 0.15 μs in width, and 1 kHz in repetition rate. In the experiment, the PZT bar with different aspect ratio R and the array transducer with different backing layer were studied. Fig. 8 shows the variation of the electrical impedance of the PZT with the driving frequency for two different aspect ratios. The acoustic impedance of the backing layer was designed as 5.6 MRayls. According to the measurement results in Fig. 8a, the difference between the thickness extensional mode and the lateral mode is approximate 4 MHz when the aspect ratio $R = 0.5$. Hence, these two modes are not coupled with each other. On the other hand, the measurement results in Fig. 8b indicate that the difference between the thickness extensional mode and the lateral mode is less than 1 MHz when the aspect ratio $R = 1.0$. In this case, these two modes could be coupled with each other. Moreover, the trend of the predicted curves agrees well with that of the experimental ones.

In application of this technique, the hammer with $R = 1.0$ would be selected as the excitation source of the microstructure in experiment. The impulse frequency response of the

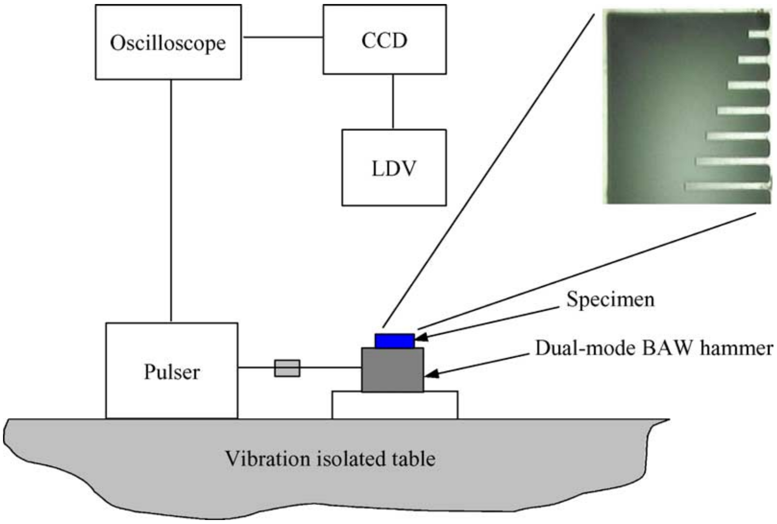

Fig. 7. The experimental setup for dual-mode BAW hammer test.

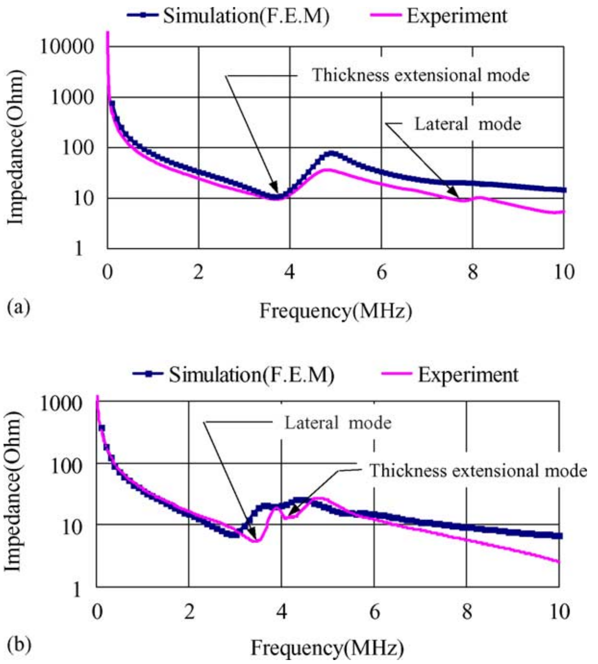

Fig. 8. Comparison of simulation and experimental results of the electrical impedance of the hammer for two different aspect ratios: (a) $R = 0.5$; (b) $R = 1.0$.

array transducer with $R = 1.0$ was also available, as shown in Fig. 9. The predicted impulse spectrum of the hammer was closely correlated to the measured one. However, the predicted frequency response was lower than the measured one. This was mainly due to the ignorance of the backing layer on the boundary of PZT during modeling. In short, the existing of backing layer added constraint on the PZT bars so as to increase their resonant frequencies.

The free vibration of the cantilever after excited by the dual-mode BAW hammer is shown in Fig. 10. The dimension of the test cantilever was 1.1 μm thick, 5.3 μm wide and 80 μm long. During the measurement, the laser spot of LDV was placed on the free end of the cantilevers. The first few cycles of the response as indicated in Fig. 10a were due to the dynamics of the dual-mode BAW hammer, but not the vibration of the beam. Afterwards, the dynamic response, which represents the free vibration of the cantilever, shows a typical viscous damped result. The measured frequency spectrum in Fig. 10b is associated with the time domain response in Fig. 10a. The results revealed that the dual-mode BAW hammer could excite the resonant frequencies of the microstructure to about 5 MHz range. Thus, various vibration modes of the beam, including four out-of-plane bending modes and one in-plane bending mode, were measured in one excitation.

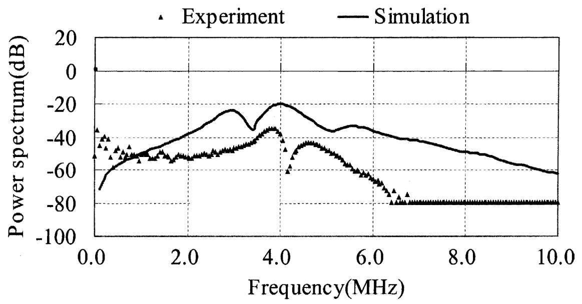

Fig. 9. Comparison of simulation and experimental results of the impulse frequency response of the hammer for $R = 1.0$.

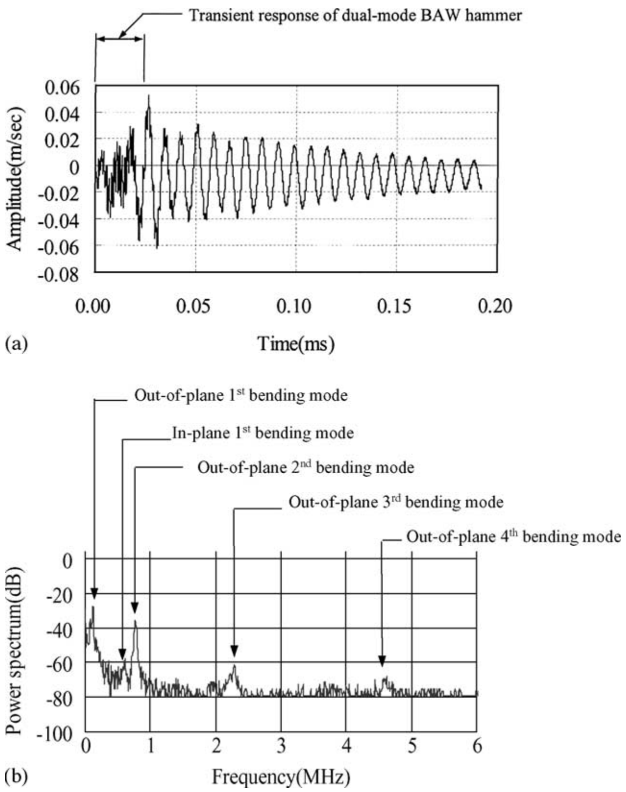

Fig. 10. The measured impulse response of the micro beams with 1.1 μm thick, 6 μm wide, and 80 μm long: (a) impulse time response; (b) impulse frequency response.

To verify the validation of the dual-mode BAW hammer technique, the comparison between the measured and predicted resonant frequencies is listed in Table 2. Apparently, the experimental results agree well with the predicted ones. The deviations between the measured resonant frequency of the out-of-plane bending modes and the predicted ones were ranging from 1.7% to 7.4%. Moreover, the in-plane Young's modulus of the sample will be determined according to the measured frequency of the in-plane bending mode.

4. Conclusion

In conclusion, a novel excitation device to determinate the in-plane and out-of-plane dynamic response of the microstructure using pulsed dual-mode ultrasonic array transducer has been demonstrated. The ultrasonic array transducer excited by the impulse signal acting as a BAW hammer to provide in-plane and out-of-plane dual-axis excitation to the testing sample. Hence, the vibration modes of the microstructure for both of the in-plane and out-of-plane directions can be excited by the BAW hammer. The in-plane and out-of-plane bending modes of the micro beam can be simultaneously measured by LDV in one pulse excitation. Experimental results agreed well with the simulation ones. Since the sample and the measurement apparatus are very simple, this approach has the potential for wafer level on-line testing.

Acknowledgements

The authors would like to express his appreciation to the BroadSound Technology Corporation (BTC), the NSC Central Regional MEMS Center (Taiwan), the Electrical Engineering Department of National Tsing Hua University (Taiwan), Semiconductor Research Center of National Chiao Tung University (Taiwan), and the NSC National Nano Device Laboratories (Taiwan) in providing experimental facilities.

References

[1] D. Certon, N. Felix, E. Lacaze, F. Teston, F. Patat, Investigation of cross-coupling in 1-3 piezocomposite arrays, IEEE Trans. Ultrasonics Ferroelectrics Freq. Control 48 (2001) 85–92.

[2] Y. Lin, J.M. Modson, J. Hamilton, J.-U. Kluiwstra, C. Cain, K. Grosh, Theory and experiment for the design of piezoelectric element for phased arrays, Proc. IEEE Ultrasonic Symp. 2 (1997) 1697–1700.

[3] R.E. McKeighen, Design guidelines for medical ultrasonic arrays, Proc. SPIE Med. Imaging 3341 (1998) 2–18.

[4] S.W. Smith, D.M. Mills, Finite element comparison of single crystal vs. multi-layer composite arrays for medical ultrasound, IEEE Trans. Ultrasonics Ferroelectrics Freq. Control 49 (7) (2002) 1015–1020.

[5] L.R. Gavrilov, J.W. Hand, P. Abel, C.A. Cain, A method of reducing grating lobes associated with an ultrasound linear phased array intended for transrectal thermotherapy, IEEE Trans. Ultrasonics Ferroelectrics Freq. Control 44 (5) (1997) 1010–1017.

[6] L. Kiesewetter, J.M. Zhang, D. Houdeau, A. Steckenborn, Determination of Young’s moduli of micromechanical thin films using the resonance method, Sens. Actuators A 35 (1992) 153–159.

[7] J.S. Burdess, A.J. Harris, D. Wood, R.J. Pitcher, D. Glennie, A system for the dynamic characterization of microstructures, J. Microelectromech. Syst. 6 (1997) 322–328.

[8] H. Majjad, S. Basrour, P. Delobelle, M. Schmidt, Dynamic determination of Young’s modulus of electroplated nickel used in LIGA technique, Sens. Actuators A 74 (1999) 148–151.

[9] W.-P. Lai, W Fang, Novel bulk acoustic wave hammer to determinate the dynamic response of microstructures using pulsed broad bandwidth ultrasonic transducer, Sens. Actuators A 96 (2002) 43–52.

[10] D. Walsh, B. Culshaw, Optically activated silicon microresonator transducers: an assessment of material properties, Sens. Actuators A 25–27 (1991) 711–716.

[11] K.B. Lee, Y.H. Cho, Electrostatic control of mechanical quality factors for surface-micromachined lateral resonators, J. Micromech. Microeng. 6 (1996) 426–430.

[12] W.C. Tang, C.T.-C. Nguyen, R.T. Howe, Laterally driven polysilicon resonant microstructure, Sens. Actuators A 20 (1989) 25–32.

[13] J. Hsieh, C.C. Chu, J.M. Tsai, W. Fang, Using extended BELST process in fabricating vertical comb actuator for optical applications, in: Proceedings of the IEEE/LEOS International Conference on Optical MEMS, Lugano, Switzerland, August 2002, Paper WP 39.

[14] N. Guo, P. Cawley, The finite element analysis of the vibration characteristics of piezoelectric discs, J. Sound Vibration 159 (1) (1992) 115–138.

Biographies

Wen Pin Lai was born in Taiwan, in 1966. He received the MS degree in Mechanical Engineering from Chung Kung University at Tainan, and the PhD degree in Power Mechanical Engineering from National Tsing Hua University at Hsinchu, Taiwan. Now he works at the BroadSound Corporation, Hsinchu, Taiwan. Meanwhile, he is engaged in the development of ultrasonic transducers for medical ultrasonic diagnostic application. His research is focus on the application of ultrasonic transducers for vibration testing of microstructures.

Weileun Fang was born in Taipei, Taiwan, in 1962. He received his PhD degree from Carnegie Mellon University in 1995. His doctoral research focused on the determining of the mechanical properties of thin films using micromachined structures. In 1995, he worked as a postdoctoral research at Synchrotron Radiation Research Center, Taiwan. He is currently an associate professor at Power Mechanical Engineering Department, National Tsing Hua University, Taiwan. His research interests include MEMS with emphasis on micro optical systems, microactuators and the characterization of the mechanical properties of thin films.